Molecular Organization in Crystalline $[Co_2(CO)_8]$ and $[Fe_2(CO)_9]$ and a Search for Alternative Packings for $[Co_2(CO)_8]$ †

Dario Braga,*[a] Fabrizia Grepioni,[a] Piera Sabatino[a] and Angelo Gavezzotti*[b]

[a] *Dipartimento di Chimica "G. Ciamician", University of Bologna, Via F. Selmi 2, 40126 Bologna, Italy*

[b] *Dipartimento di Chimica Fisica ed Elettrochimica e Centro CNR, University of Milan, Via Golgi 19, 20133 Milan, Italy*

The molecular organization in crystals of $[Co_2(CO)_8]$ and $[Fe_2(CO)_9]$ has been investigated by means of packing potential-energy calculations and computer graphic analysis. It is shown that the two molecules pack in nearly identical ways in their crystals. However, while crystalline $[Fe_2(CO)_9]$ is compact, solid $[Co_2(CO)_8]$ presents large empty channels (van der Waals width between 2.4 and 4.5 Å, at room temperature) corresponding to the approximate location of possible residual electron density (whether due to Co–Co bonding electrons or to lone pairs on the Co atoms). Alternative crystal packings for $[Co_2(CO)_8]$ have been generated, using improved atomic potential parameters adapted to carbonyl compounds. On purely steric grounds, it is shown that the $[Co_2(CO)_8]$ molecule is compatible with more close-packed crystal arrangements than the one actually observed. In two alternative triclinic and monoclinic crystal structures the 'empty' bridging sites are shown to be available for molecular interlocking.

In previous papers we have shown that much can be learnt about the properties of organometallic solids from an investigation of the factors controlling the molecular organization within their crystals.[1,2] Our approach to crystal packing has its roots in the atom–atom pairwise potential-energy method developed, and still widely used, to investigate the packing modes of organic molecules.[3] By this means we have studied the relationship between crystal packing and molecular shape of first-row transition-metal binary carbonyls[1a] and clusters,[1b] and of mononuclear metal–arene[1c] and metallocene[1d] complexes as well as the dynamic behaviour shown by a number of neutral organometallic species in the solid state.[2a,e]

This paper is devoted to an analysis of the relationship between the *crystal* and *molecular* structure of two fundamental carbonyl species, namely $[Co_2(CO)_8]$[4] and $[Fe_2(CO)_9]$.[5] These prototypical molecules have been the subject of much experimental and theoretical work, mainly because of the controversy involving the description of the bonding in $[Co_2(CO)_8]$. The effective atomic number (e.a.n.) rule in this diamagnetic compound can be satisfied either by combining two metal orbitals pointing along the metal–metal vector ('straight bond' model) or two metal orbitals directed towards the empty bridging site ('bent bond' model).[6,7] Infrared studies both in solution and in frozen matrices have revealed that $[Co_2(CO)_8]$ exists in several different isomeric forms,[8] some of which do not contain bridging carbonyls; $[Fe_2(CO)_9]$ has been less studied owing to its insolubility in most solvents.[5] More recently it was found that $[Co_2(CO)_8]$ possesses an interesting dynamic behaviour in the solid state,[9] while $[Fe_2(CO)_9]$ is static.[10] As an alternative to the ligand-exchange model put forward[9] to explain the ^{13}C cross polarization magic angle spinning (CP MAS) NMR spectra of $[Co_2(CO)_8]$ it has been suggested that librational motions of both the Co–Co axis and of the CO ligands are responsible for the observed dynamic behaviour.[11] In our earlier study[1a] we were able to show that Kitaigorodsky's packing coefficient[3] is lower in crystals of $[Co_2(CO)_8]$ than of $[Fe_2(CO)_9]$ (0.63 *versus* 0.68 at room temperature)[1a,12] indicating that the packing in $[Co_2(CO)_8]$ is less tight than in $[Fe_2(CO)_9]$, and does not prohibit the extensive swinging motion leading to apparent site exchange on the NMR time-scale.

We could also demonstrate that the molecular organization in the crystals of the two species is almost identical, in spite of the fact that $[Co_2(CO)_8]$ possesses one bridging CO less than $[Fe_2(CO)_9]$. In both lattices the reference molecule is surrounded by twelve first-neighbour molecules distributed in anticubooctahedral fashion[1a] (see Fig. 1).

Nevertheless, the factors controlling the crystal structure of $[Co_2(CO)_8]$ are still to be fully understood. The 'loose' packing may be related to the presence of 'unseen' electron density in the region of the missing ligand, or to the fact that the 'empty' bridging sites are secluded in the ligand envelope and unavailable for molecular interlocking.

In this paper we try to address this question (the 'perpetual' steric–electronic dualism) by investigating further the relationship between the experimentally observed crystal structures of $[Co_2(CO)_8]$ and $[Fe_2(CO)_9]$ and then by generating a few different, but equally efficient, crystal packings for $[Co_2(CO)_8]$, starting from molecular shape and size alone. The basic assumption is that the 'empty' bridging sites are available for molecular self-assembly.

Relationship between the Molecular Organization in Crystalline $[Co_2(CO)_8]$ and $[Fe_2(CO)_9]$

The unit cell of crystalline $[Co_2(CO)_8]$ contains two independent 'half' molecules, each of which is related to the second 'half' by a crystallographic mirror plane (space group $P2_1/m$, $Z = 4$). Two crystallographic studies have been carried out, the more recent at 100 K in order to investigate the charge density of the metal–metal bond.[4b] The compound $[Fe_2(CO)_9]$ crystallizes in the space group $P6_3/m$ with $Z = 2$.[5] Fig. 2 shows a section cut through the van der Waals envelope along the crystallographic mirror plane in the packing of the two species,

† *Supplementary data available* (No. SUP 56871, 7 pp.): lattice constants and atomic coordinates for calculated structures. See Instructions for Authors, *J. Chem. Soc., Dalton Trans.*, 1992, Issue 1, pp. xx xxv.

Non-SI unit employed: cal = 4.184 J.

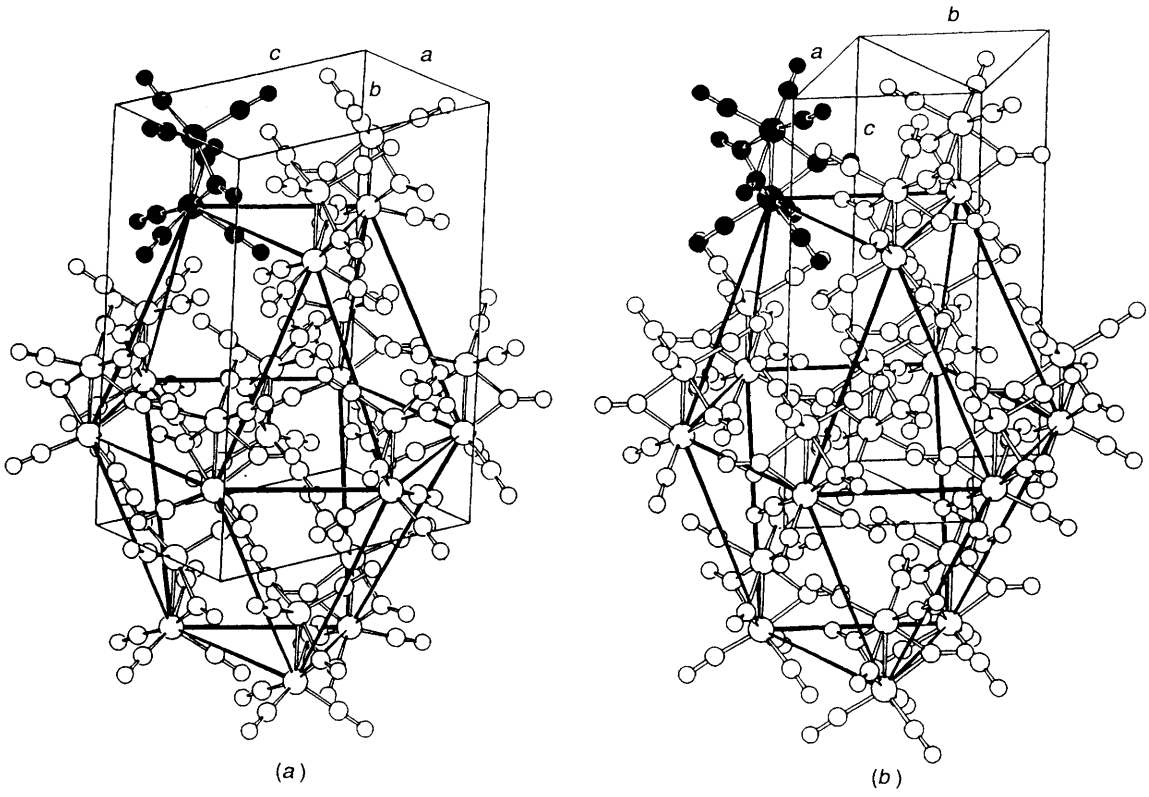

Fig. 1 The enclosure shells of $[Co_2(CO)_8]$ (*a*) and $[Fe_2(CO)_9]$ (*b*) showing the quasi-anticubooctahedral distribution of the 12 first-neighbouring molecules[1a] around the reference molecule in the experimental packings of the two species

bisecting a layer of molecules and comprising the bridging carbonyls. In spite of the differences in space-group symmetry the molecules are distributed in a similar way in the two layers. While the three bridging CO groups in $[Fe_2(CO)_9]$ are tightly interlocked with those of six surrounding molecules [see Fig. 2(*a*)], those of $[Co_2(CO)_8]$ show two different kinds of interactions. Molecules belonging to row A [see Fig. 2(*b*)] interact on one side with those of row B *via* insertion of one bridging CO in between two bridging CO groups of the neighbouring molecules, as in $[Fe_2(CO)_9]$; on the opposite side the unbridged sites of the molecules belonging to rows A and C face each other. This packing distribution results in *rather large continuous channels* along the *a* axis in the lattice of $[Co_2(CO)_8]$ (van der Waals width from packing-density maps in the range 2.4–4.5 Å), accounting for the difference in packing coefficients between the two crystals. Interestingly the distance between row A and row B is *smaller* than the distance between rows A and C (intermolecular separation between parallel Co–Co vectors *ca.* 5.29 *versus* 5.82 Å). The channels are delimited along the *b* axis by the $(CO)_3$ umbrellas, as shown in Fig. 3. The interlocking between terminal tricarbonyl units of neighbouring molecules is shown in Fig. 4 for $[Co_2(CO)_8]$: the dimples originating in three terminal CO groups of one layer of molecules are filled by the $(CO)_3$ units of a second layer. At this stage one might wonder why $[Co_2(CO)_8]$ has not adopted a more efficient interlocking pattern in order to better fulful the requirements of the close-packing principle.[3a] As mentioned in the Introduction one possibility (the '*electronic* approach') is that the channels indeed accommodate the electron density from the cobalt orbitals pointing towards the 'missing ligands'. This electron density should be very diffuse and polarizable, giving rise to van der Waals type interactions that contribute to the crystal stability. On this premise the effective molecular shapes of $[Fe_2(CO)_9]$ and $[Co_2(CO)_8]$ would be very much the same, accounting for the similarity between the two packings. The other possibility (the '*steric* approach') is two-fold: either the crystal packing is governed by the interactions among the terminal CO groups (*e.g.* a more efficient interlocking of the bridging ligands would lead to loss of cohesion among the terminal ones), or the unoccupied bridging sites cannot be efficiently used by neighbouring molecules for intermolecular interlocking.

In order to throw light on this problem, we have generated some alternative crystal structures for $[Co_2(CO)_8]$, seeking possible ways to pack the same molecule without cavities or channels in the lattice. The best candidates for this purpose will be those molecular arrangements in which the crystal packing takes full advantage of the space left by the 'missing' ligand in order to optimize intermolecular interlocking. The procedure we adopt amounts to crystal structure prediction starting from molecular structure alone, a task that has seldom been attempted for organic molecules (see, for example, ref. 13) and never for organometallic ones; on the experimental side, the possible occurrence of polymorphic organometallic crystals has never been systematically explored.

Crystal Potentials

A comparison of the packing energies for the same compound in different crystal structures will be necessary in the following discussion; the choice of appropriate crystal potentials is therefore important. Use will be made in this work of the atom–atom potential method,[3] where the crystal energy, or packing potential energy (p.p.e.), is written as in equation (1) where r_{ij}

$$\text{p.p.e.} = \Sigma_i\Sigma_j\{A\exp(-Br_{ij}) - Cr_{ij}^{-6} + [(q_iq_j)/r_{ij}]\} \quad (1)$$

represents the non-bonded atom–atom intermolecular distance and q the atomic charge. Index i in the summation encompasses all atoms of the reference molecule, and index j all the atoms of the surrounding molecules distributed according to crystal symmetry. In previous work,[1,2] where absolute values for the lattice energy were less crucial, the method was applied in a

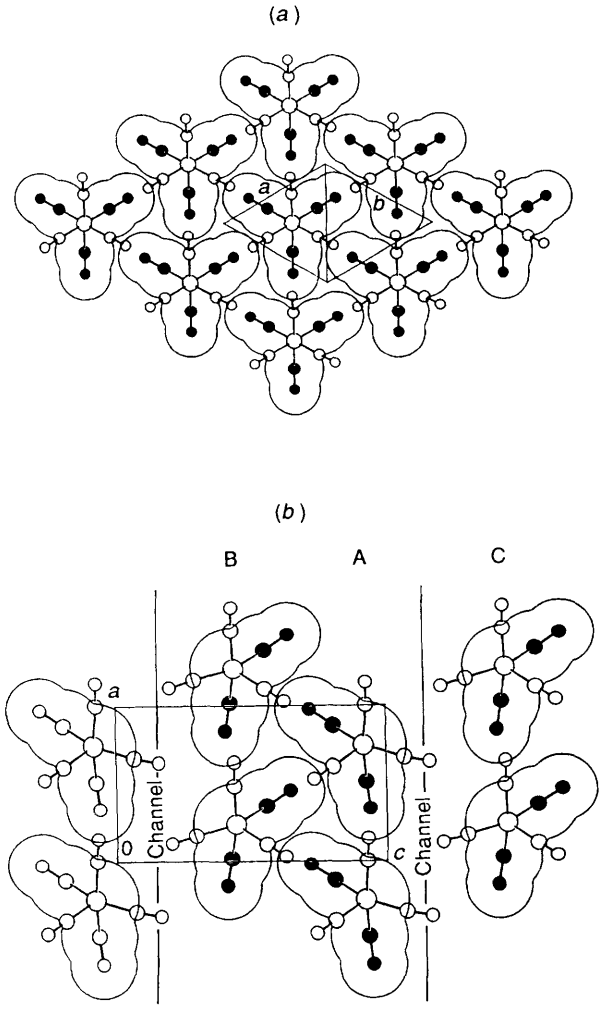

Fig. 2 Sections of the crystal packings of $[Fe_2(CO)_9]$ (*a*) and $[Co_2(CO)_8]$ (*b*) along the crystallographic mirror plane. The molecular axes are perpendicular to the grid plane. Van der Waals outlines and filled atom spheres correspond to the bridging carbonyls. (*a*) Each group of bridging carbonyls is tightly interlocked among six other groups; (*b*) rows A and B interact *via* insertion of CO between two neighbouring bridging CO groups. Rows A and C offer each other the unbridged sites leaving 'empty' channels along the *a* axis

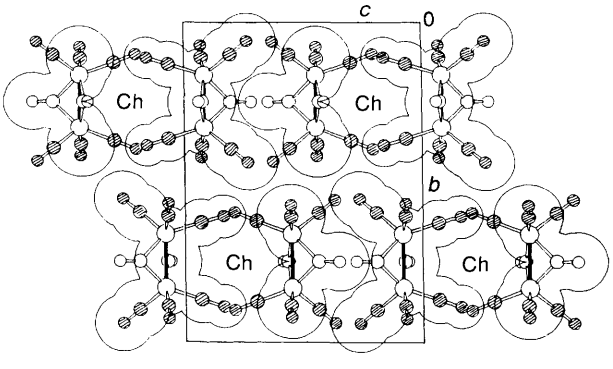

Fig. 3 Section of the $[Co_2(CO)_8]$ packing perpendicular to the channels (Ch) shown in Fig. 2(*b*). The channels are delimited along the *b* axis by the terminal tricarbonyl units (shaded atoms)

simplified form, neglecting the r^{-1} term; parameters *A*, *B* and *C* were taken from Mirsky,[14] and a cut-off of 10 Å was imposed on the lattice sums; we call this scheme M10. More accurate parameters for some oxohydrocarbons have been proposed by Williams and co-workers,[15] including contributions from the r^{-1} term, where the q_i are atomic charges to be determined by quantum-chemical methods. In this scheme, convergence of the lattice sums is ensured, so we call it Coulomb–Convergent–Williams, or CCW. With both schemes some choice for the metal-atom potentials must be made; in the CCW scheme one also has to provide site charges for carbon and oxygen.

To tackle these problems we have run test calculations on the observed crystal structure for $[Co_2(CO)_8]$, using a computer program (PCK 83[16]) that allows the optimization of cell parameters and molecular rigid-body rotation and translation, under the action of a given crystal potential (structure 'relaxation'). The results shown in Table 1 clearly demonstrate that: (*i*) the choice of the parameters for the metal atom is irrelevant, (*ii*) when site charges are neglected, Mirsky and Williams potentials give quite similar results, and (*iii*) the inclusion of a small dipole on the carbonyls is necessary to avoid modifications of the observed structure. The setting which produces the smallest displacements from the observed structure uses a dipole charge of 0.2 e^-. In the following discussion, therefore, calculations labelled CCW include metal atoms treated as hydrogens and a dipole charge of 0.2 e^-.

Search for Alternative Crystal Packings for $[Co_2(CO)_8]$

In this search we used a procedure[17] in which the most common symmetry operators (in our case, the inversion centre *I* and the screw diad *S*) are used to construct multimolecular nuclei, which are then translated in the three directions in space to provide a number of trial crystal structures in the most frequent space groups ($P\bar{1}$, $P2_1$, $P2_1/c$, $P2_12_12_1$; more symmetrical space groups result from molecular point-group symmetry). The first stages of this search, that is the generation of the nuclei and the preliminary location of potential-energy valleys, were carried out within the M10 approximation to save computing effort; the most promising structures thus obtained were then subjected to full optimization using the refined CCW scheme. Meaningful energy comparisons were then made between each calculated structure and the optimized experimental structure, that is between fully relaxed structures. The complete results of the structure search are shown in Table 2, and are described in more detail in the following. Tables of unit-cell dimensions and fractional atomic coordinates for all calculated crystal structures listed in Tables 2 and 3 for $[Co_2(CO)_8]$ and $[Fe_2(CO)_9]$ are available as SUP 56871.

I Nucleus.—There are essentially two ways to interlock efficiently two molecules of $[Co_2(CO)_8]$ *via* an inversion centre. These have been identified as bridge–bridge (BB) and bridge–terminal (BT) modes. In the BB mode the two sets of bridging CO groups are coplanar. This arrangement locates the two empty bridging sites on the opposite sides of the nucleus [Fig. 5(*a*)]. In the BT mode the two molecules are offset by about half the Co–Co length, so that two terminal CO groups from one $(CO)_3$ unit 'embrace' the empty bridging site [Fig. 5(*b*)].

Starting from these two nuclei several possible triclinic cells (see Table 2) can be generated by the translational search and optimization procedure. Structures labelled **IA** and **IB** (based on the BB mode) are very similar, and contain the channels. In structure **ID** [also based on the BB mode, see Fig. 6(*a*)] channels are no longer present, while cavities are formed between contiguous centrosymmetric nuclei that offer each other the 'empty' bridging sites.

Far more interesting is structure **IC**, based on the BT mode. As shown in Fig. 6(*b*), pairs of terminal CO groups belonging to one row of molecules fold around the Co–Co axes of molecules belonging to an adjacent row. Close packing is achieved, no channels or cavities are present. This structure has the highest packing energy among the calculated ones for space group $P\bar{1}$.

S Nucleus.—As for the inversion centre, there are only a few

Table 1 Test calculations on the observed crystal structure of $[Co_2(CO)_8]$

Parameter set[a]	Metal treated as	Dipole charge/e$^-$	p.p.e.[b]	Cell parameter variations a/Å	b/Å	c/Å	β/°	Δθ[c]/°	Δx[d]/Å
W	C	0.3	56.3	−0.19	−0.32	−0.32	0.8	1.7	0.15
								1.3	0.29
W	C	0.0	35.1	0.35	−0.34	−0.83	0.0	11.6	0.48
								12.8	0.56
W	H	0.3	50.7	−0.15	−0.28	−0.26	0.8	1.7	0.15
								1.3	0.29
W	H	0.2	38.1	0.0	−0.20	−0.27	0.5	3.1	0.11
								1.7	0.14
W	H	0.0	30.0	0.39	−0.28	−0.75	0.0	11.6	0.48
								12.8	0.56
M	H	—	29.7	0.29	−0.48	−0.92	0.1	11.2	0.42
								12.4	0.46
M	C	—	34.0	0.26	−0.52	−0.98	0.1	11.2	0.40
								12.4	0.44
M	Kr	—	46.5	0.20	−0.62	−1.15	0.1	11.5	0.36
								12.7	0.47

[a] W = Williams, M = Mirsky. [b] Packing potential energy after structure relaxation in the crystal field. [c] Total rigid-body rotational displacement. [d] Total rigid-body translational displacement after relaxation. Two values are given, one for each of the two molecules in the asymmetric unit.

Table 2 Observed and calculated crystal structures for $[Co_2(CO)_8]$

	M10			CCW								
Structure label	V_{cell}/Å^3	C_K[a]	p.p.e.[b]	V_{cell}/Å^3	C_K[a]	p.p.e.[b]	a/Å	b/Å	c/Å	α/°	β/°	γ/°
X-Ray unoptimized	2 × 583.7	0.63	39.4	—	—	—	6.62	15.59	11.31	—	90.00	—
X-Ray optimized	2 × 518.6	0.71	46.5	2 × 562.4	0.65	38.1	6.618	15.39	11.04	—	90.52	—
I Nucleus space group $P\bar{1}$												
IA	560.3	0.66	40.4	584.8	0.63	34.0	6.515	8.800	11.350	105.5	105.7	99.1
IB	563.3	0.66	40.3	586.3	0.63	33.9	6.491	9.518	11.09	105.6	98.8	107.3
IC	565.0	0.65	40.0	579.9	0.63	34.9	6.528	8.285	11.32	82.1	83.8	79.5
ID	554.0	0.67	41.3	585.4	0.63	33.8	7.017	8.416	11.21	96.2	103.5	111.5
S Nucleus space group $P2_1$												
SA	568.6	0.65	40.0	583.9	0.63	34.5	8.322	6.501	11.22	—	105.9	—
SB	539.4	0.69	42.0	568.0	0.65	36.8	6.724	6.419	13.22	—	95.3	—
SC	553.2	0.67	41.0	578.0	0.64	36.3	8.275	6.494	10.76	—	91.9	—

[a] Packing coefficient calculated with R_{Co} = 2.15 Å. [b] In kcal mol^{-1}. For M10, Co as krypton.

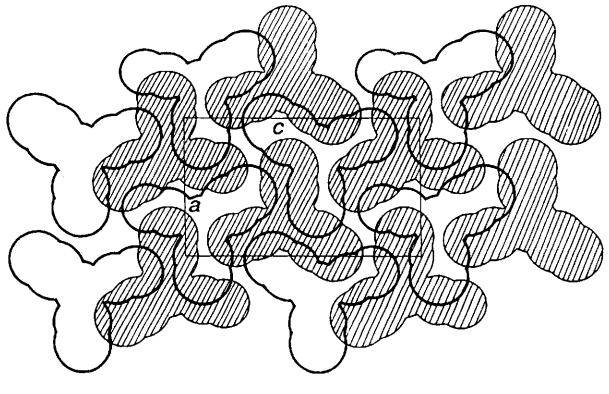

Fig. 4 Grid-cutting of the $[Co_2(CO)_8]$ packing perpendicular to the *b* axis, showing how the tricarbonyl units of one layer of molecules (shaded van der Waals outlines) are accommodated over the dimples of the tricarbonyl units of a second molecular layer (thick outlines)

possibilities to interlock efficiently the molecules *via* a two-fold screw operator. Fig. 7(*a*) (structure **SA**, Table 2) shows the packing generated by a 2_1 axis perpendicular to the Co–Co bonds and roughly parallel to the C–O axis of one bridging CO of molecule **SA1**. This results in one bridging CO of molecule **SA2** pointing towards the middle of the bridging $(CO)_2$ unit of molecule **SA1**. The molecular rows generated by translational symmetry form channels which closely recall those observed in the experimental packing [compare Figs. 7(*b*) and 3], although the separation between rows decreases slightly (compare 5.28 and 5.58 Å in **SA** with 5.29 and 5.82 Å in the experimental structure). Thus our procedure for crystal-structure generation has retraced the observed crystal structure, although in a different framework. In fact the 2_1 axis in the experimental structure is perpendicular to the plane containing the bridging ligands, while in the calculated one it lies in that plane (cell axis relationship: $a' \approx b/2$, $b' \approx a$, $c' \approx c$, $\beta' = 105.9$, $\beta = 90.0°$, primed for structure **SA**, see Table 2).

The packing shown in Fig. 8(*a*) (structure **SB** in Table 1) is the most interesting one. As shown in Table 2 the packing coefficient in the case of **SB** is equal to that of the experimental structure (after CCW optimization). The key interaction is observed between molecules related by translational symmetry [see Fig. 8(*a*)]. The interlocking pattern is based on the insertion of one terminal ligand right in between the four terminal ligands surrounding the empty bridging site of an adjacent molecule [see Fig. 8(*b*)]. A similar interlocking mode is shown by structure **SC**, although the terminal–tetragonal interaction is generated by the 2_1 axis and not by translational symmetry. Structures **SB** and **SC** are, therefore, two other examples of structures in which the channels are no longer present and close packing is achieved by 'making use' of the empty bridging sites

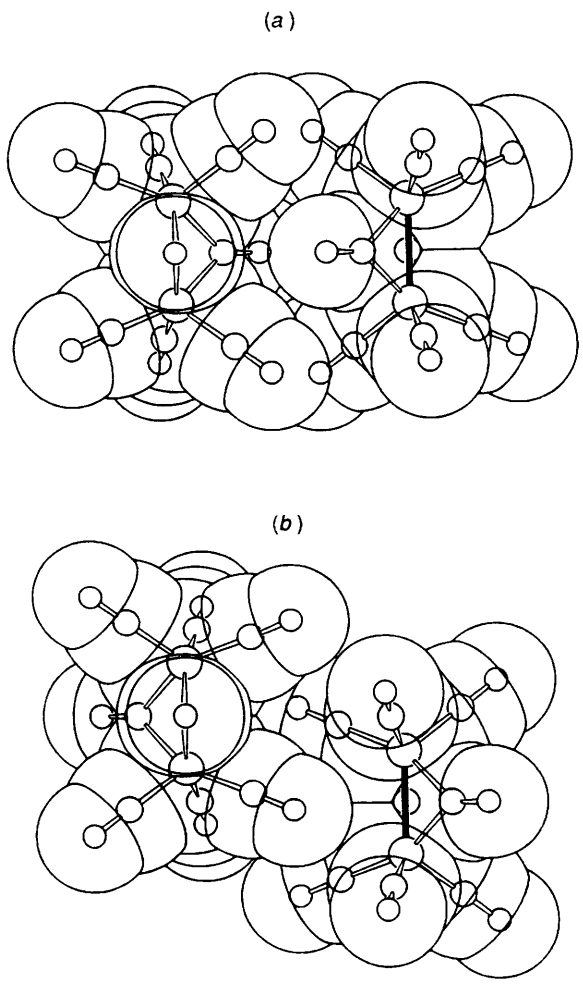

Fig. 5 The *I* nuclei obtained for $[Co_2(CO)_8]$ from the search procedure: (*a*) BB mode where the two sets of bridging carbonyls are coplanar and the 'empty' bridging sites are located on the opposite sides of the nucleus; (*b*) BT mode where two terminal carbonyls of one molecule embrace the 'empty' bridging site of a neighbouring molecule

Structure Search for $[Fe_2(CO)_9]$

As a further test of the structure-generation procedure and of the crystal potentials a search in space group $P\bar{1}$ has also been conducted for $[Fe_2(CO)_9]$; Table 3 shows some of the results. Among the calculated triclinic crystals for this molecule, the unit-cell parameters of structure **II** (see Table 3) closely approximate the cell edges and angles of the experimental trigonal cell of $[Fe_2(CO)_9]$. Fig. 9 shows how the molecular interlocking pattern observed in the experimental crystal structure of $[Fe_2(CO)_9]$ [Fig. 2(*a*)] is reproduced in this triclinic cell; the packing coefficients in the observed and calculated structure are also strictly comparable. The other triclinic structure (**IF**) calculated for $[Fe_2(CO)_9]$ is also densely packed. Some other $P2_1$ structures were generated for this compound, but were invariably less stable than the observed one.

Discussion

In our analysis of the crystal energetics of these prototypical carbonyl compounds we have demonstrated that the inclusion of a dipole charge for CO gives better results, while the effective potentials used for the metal atoms only produce shifts of absolute values, but leave energy differences unchanged. In Table 1 it seems that all calculations not including charges give large displacements from the observed crystal structure, while using H, C or Kr potentials for the metal has the same effect on the displacement, although absolute values for the packing

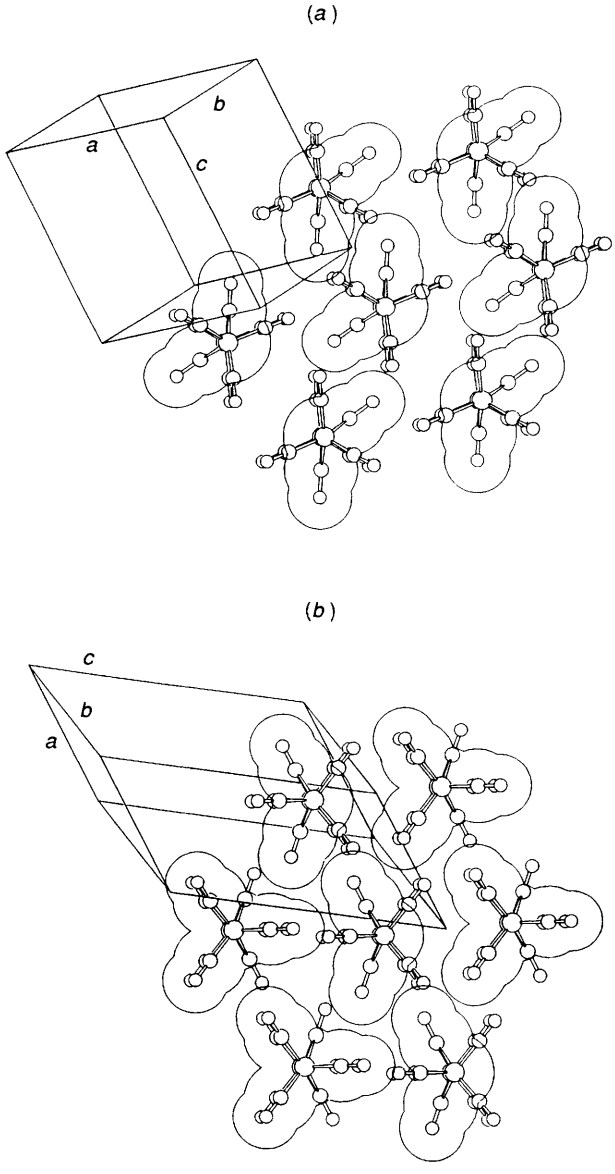

Fig. 6 Triclinic $[Co_2(CO)_8]$ crystals. Sections through the bridging unit of the central molecule: (*a*) structure **ID** based on the **BB** mode (this packing leaves cavities in the lattice); (*b*) structure **IC** based on the **BT** mode (neither cavities nor channels are left in the packing)

energy are different. A quantitative calibration of the parameters for the metal atom would require an experimental value for the sublimation energy. The M10 parametrization is quite sufficient for the identification of the main energy valleys, and also gives a preliminary appreciation of energy ordering; for instance, the most stable of the calculated crystal structures for $[Co_2(CO)_8]$, **SB** in Table 2, is such according to both M10 and CCW parameters.

The structure-search procedure proved reliable, since the observed crystal structures for both compounds have been traced, and the results are even more convincing since they have been obtained without using the full space-group restrictions. The search in $P2_1$ for the cobalt compound has regenerated the mirror plane existing in the observed crystal structure; the trigonal structure of the iron compound was traced by the search in $P\bar{1}$, the equality of the *a* and *b* cell edges and the fixed values for the cell angles having been approached very closely. Small differences, however, remain; this is slightly disturbing, since it means that the potential-energy surface, even close to the minimum, is not smooth and must have sub-minima.

The results so far discussed are mainly of methodological

Table 3 Observed and calculated crystal structures for $[Fe_2(CO)_9]$ *

	M10			CCW								
Structure label	V_{cell}/Å^3	C_K	p.p.e.	V_{cell}/Å^3	C_K	p.p.e.	a/Å	b/Å	c/Å	α/°	β/°	γ/°
X-Ray unoptimized	578.4	0.68	47.5	—	—	—	6.436	6.436	16.123	90	90	120
X-Ray optimized				577.9	0.68	45.5	6.470	6.470	15.940	90	90	120
I Nucleus space group $P\bar{1}$												
IF	581.3	0.68	47.3	605.4	0.65	41.3	6.407	8.405	12.473	98.2	104.4	107.0
II	567.5	0.69	47.2	591.1	0.67	42.4	6.452	6.458	16.49	93.9	94.0	119.7

* See footnote to Table 2 for units.

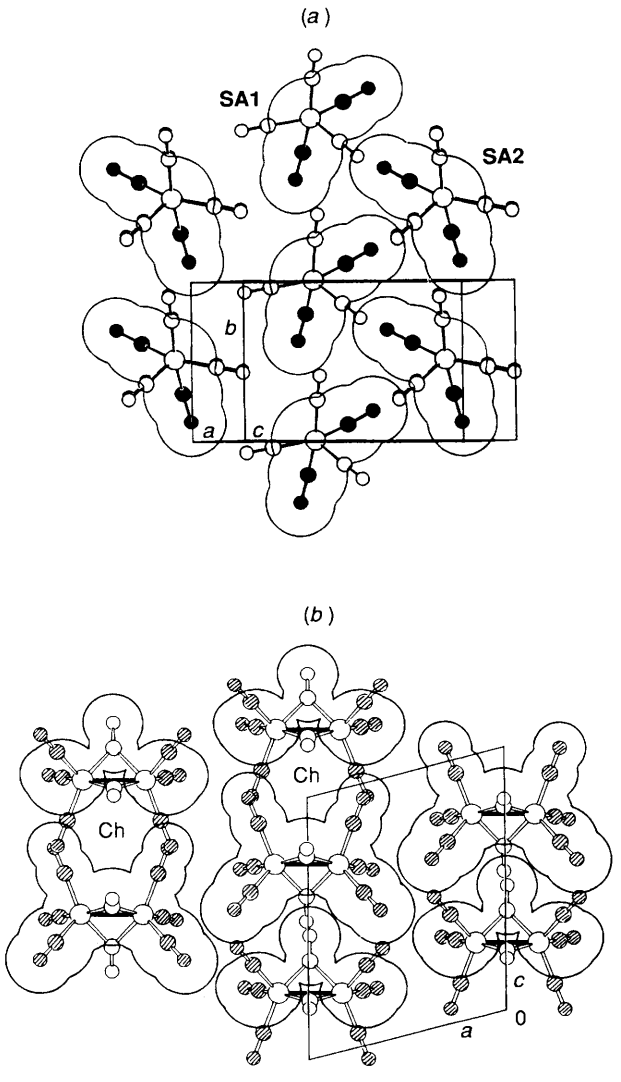

Fig. 7 Monoclinic $[Co_2(CO)_8]$ crystals: (*a*) a section cut through the bridging carbonyls of structure **SA** [compare this packing arrangement with that shown in Fig. 2(*b*); the channels extend along the *b* axis]; (*b*) a section cut perpendicular to the channels in structure **SA**. The channels are delimited by the terminal tricarbonyl units (shaded atoms) as in the experimental packing (compare with Fig. 3)

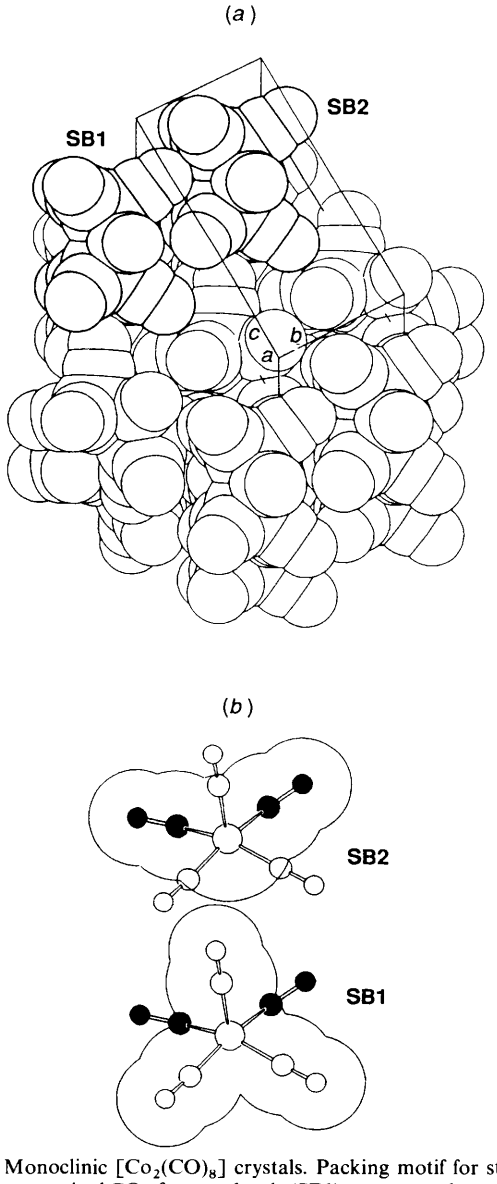

Fig. 8 Monoclinic $[Co_2(CO)_8]$ crystals. Packing motif for structure **SB**: (*a*) one terminal CO of one molecule (**SB1**) penetrates the tetragonal unit of a neighbouring molecule (**SB2**) (**SB1** and **SB2** are related by translational symmetry); (*b*) section through the bridging carbonyls of molecule **SB2** in structure **SB**, showing how the empty bridging site is filled in by the terminal CO of molecule **SB1**

importance. The results which are relevant to the particular crystal-chemistry problem outlined in the Introduction will now be discussed. The presence of channels in the crystal structure of $[Co_2(CO)_8]$ might allow inclusion and/or diffusion of small molecules like H_2, CO or HCCH. No such observations have been reported thus far for simple metal carbonyls, while the formation of inclusion compounds is rather commonplace with larger organometallic and organic molecules.[18] Potential-energy calculations have been carried out for guest H_2 or acetylene molecules, optimizing their orientation in the unrelaxed host matrix. Dihydrogen can travel along the channel with a maximum activation energy of 3.5 kcal mol^{-1}; an acetylene molecule can lodge in the host crystal with an energy loss of *ca.* 20 kcal mol^{-1}. The destabilizing interactions arise from very few short interatomic contacts, which could easily

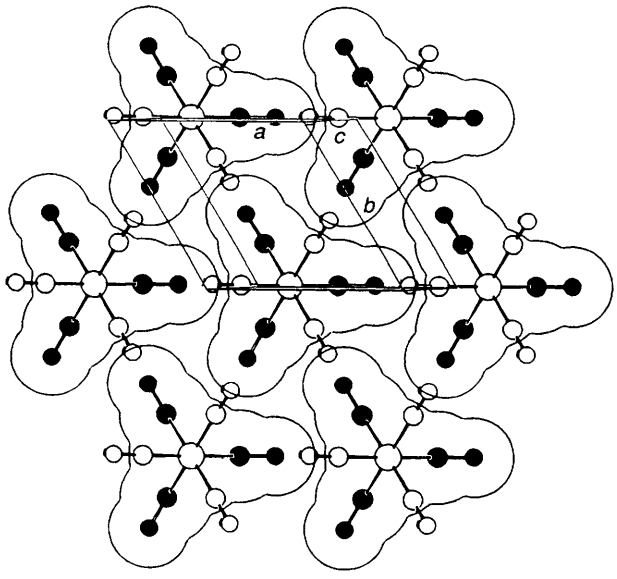

Fig. 9 Triclinic $[Fe_2(CO)_9]$ crystals. Section through the bridging carbonyls of the central molecule in structure **II** [compare with Fig. 2(*a*)]

disappear after slight readjustment of the host matrix. According to these results the inclusion and diffusion of small molecules in the $[Co_2(CO)_8]$ crystal is very likely. It would be interesting to check this prediction against experiment.

The crystal-structure search for $[Co_2(CO)_8]$ yielded several structures whose packing coefficient and packing energy are higher than those of the unrelaxed, or quite similar to those of the relaxed, experimental structure. We consider this result as strongly indicative of the possible existence of polymorphic forms for that molecule. Among them are two crystal structures in which full advantage is taken of the empty bridging sites over the molecular structure, thus demonstrating that the shape of this molecule is indeed compatible with a dense crystal packing in which this site is used for molecular interlocking.

We have previously shown[1b] that the key intermolecular interaction in the crystal packing of $[Ru_3(CO)_{12}]$ is based on the insertion of one carbonyl group in the middle of the cavity generated by four carbonyls bound to an edge of the ruthenium triangle, as we have found to occur in structure **SB** discussed above. Thus, such an interaction might be a recurrent feature in the packing of these polynuclear metal carbonyls.

Why it is that this interlocking mode is not adopted in the available crystal structure of the cobalt compound cannot be safely discerned at this stage. Our calculations allow a difference of 1.3 kcal mol^{-1} between the channel structure and the interlocking one, but it is doubtful that the empirical potentials employed here are suitable for such subtle discriminations. The matter is further complicated by the possible appearance of multi-minima potential surfaces, as previously discussed. The possibility of a subtle balance between CO · · · CO interactions (the steric hypothesis) cannot be ruled out, nor can it be excluded that some residual electron density in the molecular niche of $[Co_2(CO)_8]$, not accounted for in our calculations, plays a significant role for intermolecular interactions (according to the electronic hypothesis).

It should also be noted that none of our considerations includes entropy effects since there is no simple method for the evaluation of the entropy differences between ordered crystal phases. A crystal-structure study of $[Co_2(CO)_8]$ well below liquid-nitrogen temperature is highly desirable, since this would allow a more accurate determination of the electron density, and would reduce entropy effects.

In conclusion, we believe that the chances of finding a low-temperature or high-pressure polymorph similar to our interlocking crystal structure are substantial. The approach employed here applies to many organometallic solid-state problems. For example, it could be helpful in the determination of crystal structures from powder diffraction data, or in the prediction of ordered polymorphic modifications for some other fundamental binary carbonyls, $[Fe_3(CO)_{12}]$, $[Co_4(CO)_{12}]$ and $[Ir_4(CO)_{12}]$, for which only disordered crystal structures have so far been observed.

Acknowledgements

Financial support by Ministero dell'Università e della Riccerca Scientifica e Tecnologica is acknowledged.

References

1 (*a*) D. Braga, F. Grepioni and P. Sabatino, *J. Chem. Soc., Dalton Trans.*, 1990, 3137; (*b*) D. Braga and F. Grepioni, *Organometallics*, 1991, **10**, 1254; (*c*) D. Braga and F. Grepioni, *Organometallics*, 1991, **10**, 2563; (*d*) D. Braga and F. Grepioni, *Organometallics*, in the press.
2 (*a*) D. Braga, C. Gradella and F. Grepioni, *J. Chem. Soc., Dalton Trans.*, 1989, 1721; (*b*) D. Braga, F. Grepioni, B. F. G. Johnson, J. Lewis and M. Martinelli, *J. Chem. Soc., Dalton Trans.*, 1990, 1847; (*c*) S. Aime, D. Braga, R. Gobetto, F. Grepioni and A. Orlandi, *Inorg. Chem.*, 1991, **30**, 951; (*d*) D. Braga, F. Grepioni, B. F. G. Johnson, H. Chen and J. Lewis, *J. Chem. Soc., Dalton Trans.*, 1991, 2559; (*e*) D. Braga, F. Grepioni and E. Parisini, *Organometallics*, 1991, **10**, 3735.
3 (*a*) A. I. Kitaigorodsky, *Molecular Crystals and Molecules*, Academic Press, New York, 1973; (*b*) A. J. Pertsin and A. I. Kitaigorodsky, *The Atom–Atom Potential Method*, Springer, Berlin, 1987; (*c*) A. Gavezzotti and M. Simonetta, *Chem. Rev.*, 1981, **82**, 1; (*d*) A. Gavezzotti, *J. Am. Chem. Soc.*, 1983, **105**, 5220.
4 (*a*) G. G. Sumner, H. P. Klug and J. E. Alexander, *Acta Crystallogr.*, 1964, **17**, 732; (*b*) P. C. Leung and P. Coppens, *Acta Crystallogr., Sect. B*, 1983, **39**, 535.
5 F. A. Cotton and J. M. Troup, *J. Chem. Soc., Dalton Trans.*, 1974, 800.
6 P. Coppens, *Coord. Chem. Rev.*, 1985, **65**, 285; P. S. Braterman, *Struct. Bonding (Berlin)*, 1983, **10**, 57; C. W. Bauschlisher, *J. Chem. Phys.*, 1986, **84**, 872; W. Heijer, E. I. Baeredens and P. Ros, *Faraday Symp. Chem. Soc.*, 1980, **14**, 211; see also C. Mealli and D. M. Proserpio, *J. Organomet. Chem.*, 1990, **386**, 203 and refs. therein.
7 A. A. Low, K. L. Kunze, P. J. MacDougall and M. B. Hall, *Inorg. Chem.*, 1991, **30**, 1079.
8 R. L. Sweany and T. L. Brown, *Inorg. Chem.*, 1977, **16**, 415.
9 B. E. Hanson, M. J. Sullivan and R. J. Davis, *J. Am. Chem. Soc.*, 1984, **106**, 251.
10 H. C. Dorn, B. E. Hanson and E. Motell, *J. Organomet. Chem.*, 1982, **224**, 181.
11 D. Braga, C. E. Anson, A. Bott, B. F. G. Johnson and E. Marseglia, *J. Chem. Soc., Dalton Trans.*, 1990, 3517; C. E. Anson, R. E. Benfield, A. W. Bott, D. Braga and E. Marseglia, *J. Chem. Soc., Chem. Commun.*, 1988, 889.
12 D. Braga and F. Grepioni, *Acta Crystallogr., Sect. B*, 1989, **45**, 378.
13 G. R. Desiraju and A. Gavezzotti, *J. Chem. Soc., Chem. Commun.*, 1991, 621.
14 K. Mirsky, *Computing in Crystallography, Proceedings of the International Summer School on Crystallographic Computing*, Delf University Press, Twente, 1978, p. 169.
15 S. R. Cox, L. Y. Hsu and D. E. Williams, *Acta Crystallogr., Sect. A*, 1981, **37**, 293.
16 D. E. Williams, PCK 83, A Crystal Molecular Packing Analysis Program, Quantum Chemistry Program Exchange no. 481, Indiana University, Bloomington, IN, 1983.
17 A. Gavezzotti, *J. Am. Chem. Soc.*, 1991, **113**, 4622.
18 *Inclusion Compounds*, eds. J. L. Atwood, J. E. D. Davies and D. D. MacNicol, Academic Press, New York, 1984.

Received 20*th September* 1991; *Paper* 1/04865A